1988-06-01

Kelvin Wave-CISK: A Possible Mechanism for the 3050 Day Oscillations

Chang, C-P.; Lim, H.

AMS

Chang, CPt, and H. Lim. "Kelvin wave-CISK: A possible mechanism for the 3050 day oscillations." Journal of the Atmospheric Sciences 45.11 (1988): 1709-1720.
http://hdl.handle.net/10945/61411

Kelvin Wave-CISK: A Possible Mechanism for the 30–50 Day Oscillations*

C.-P. CHANG

Department of Meteorology, Naval Postgraduate School, Monterey, California

H. LIM

Department of Physics, National University of Singapore, Singapore

(Manuscript received 20 October 1987, in final form 5 January 1988)

ABSTRACT

Two categories of theories have been proposed to explain the observed tropical intraseasonal oscillations whose main periodicity is between 30–50 days: (i) those based on eastward propagating Kelvin waves maintained by cumulus heating; and (ii) those based on interactions with stationary oscillations of the basic state. Recent numerical modeling studies have simulated certain important aspects of the oscillations, particularly the slower propagation speed as compared with the normal Kelvin waves. Motivated by these results which lend support to the first category, a linear theoretical analysis of the equatorial β-plane wave-CISK was carried out with a focus on the Kelvin modes.

Our results show that two types of CISK modes may arise from an interaction of vertical modes. For heating with a maximum in the lower troposphere, the instability is due to the lowest internal mode which gives a stationary, east–west symmetrical structure. When heating is maximum in the midtroposphere, eastward propagating CISK modes resembling the observed and numerically-simulated oscillations occur. These modes result from the interaction between two internal modes which are locked in-phase vertically. A time-lagged CISK analysis suggests that the shallower mode, with its stronger influence on the low-level moisture convergence, slows down the deeper mode resulting in a combined mode which has a deep vertical structure with a relatively slow propagating speed. This slower phase speed may also be understood from the consideration of two effects: a CISK growth effect which is analogous to a viscous effect, and the reduction in effective static stability. A single mode analysis also suggests that the Rossby modes are less likely to become unstable. The results further imply that, in the absence of wave-CISK, the observed oscillation cannot be excited by stationary oscillations.

1. Introduction

The eastward propagating 30–50 day oscillations in the tropical atmosphere were first observed by Madden and Julian (1971, 1972) about 15 years ago. Recently, there have been many more reports of these oscillations, mainly in the monsoon flows (e.g., Yasunari 1979; Maruyama 1982; Krishnamurti and Subrahmanyan 1983; Krishnamurti et al. 1985; Murakami et al. 1984; Murakami and Nakazawa 1985; Lau and Chan 1985, 1986; Madden 1986). These studies have established that 30–50 day oscillations constitute a major component of the intraseasonal variability of the tropical atmospheric circulation.

Although two categories of theories have been proposed to explain the 30–50 day oscillations, theoretical understanding of the phenomena is still inadequate. The first category interprets the oscillations as eastward propagating Kelvin waves. Since the traditional equatorial wave theory (Lindzen 1967) predicts very short vertical wavelengths for slow propagation speeds, a theory in this category must resolve the apparent discrepancy with the deep vertical structure of the observed oscillations. An earlier attempt was made by Chang (1977), who showed that when cumulus heating and dissipation effects are taken into account, a deep Kelvin wave mode with slow propagation speed arises because of a balance between heating and dissipation. This slow Kelvin mode exhibits a northwest–southeast (northeast–southwest) phase tilt in the Northern (Southern) Hemisphere, and hence appears to agree with the often observed poleward propagation. From the point of view of CISK theory, Chang's (1977) viscous Kelvin modes may be regarded as a sort of CISK mode in which the heating is so distributed that the CISK energy generation is exactly balanced by dissipation. However, no mechanism for realizing the required heating distribution was suggested in that paper.

The second category of theories considers the oscillations as a result of excitations of slow eigenmodes of the basic state. Webster (1983) showed that a quasi-

* Preliminary results presented at the International Conference on Monsoon and Mesoscale Meteorology, Taipei, November 1986.

Corresponding author address: Dr. C. P. Chang, Dept. of Meteorology, Code 63, Naval Postgraduate School, Monterey, CA 93943-5100.

fortnightly oscillation can result from a land–sea hydrological cycle in a monsoon model; Goswami and Shukla (1984) found that interactions between convection and a zonally symmetric circulation can lead to intraseasonal oscillations; Yamaguta and Hayashi (1984), Salby and Garcia (1987) and Garcia and Salby (1987) considered the response to localized low-frequency heating and found a transient Walker circulation which resembles the 30–50 day oscillations; and Anderson and Stevens (1987) discovered several low-frequency modes in a zonally symmetric Hadley circulation. However, these studies generally do not explain the observed asymmetry that only an eastward propagation is sustained.

Two recent global numerical modeling studies, Lau and Peng (1987) and Hayashi and Sumi (1986), provided interesting insight into the phenomena which lends strong support to the view of propagating Kelvin waves. In their model simulation, CISK-type latent heating leads to the formation of self-sustained equatorial disturbances, which propagate eastward at a speed of about 20 m s^{-1}. The zonal scale of the circulation is predominantly wavenumber one, but the upward motion and convective heating are concentrated to a longitudinal interval of $\leq$3000 km. These disturbances have overall features that resemble those of the observed 30–50 day oscillations. Their gross structure strongly suggests that they are related to the propagating Kelvin waves, although their propagating speed, which is somewhat faster than observed, is much slower than those of the free Kelvin waves of similar vertical scales.

Both Lau and Peng (1987) and Hayashi and Sumi (1986) identified these disturbances as Kelvin wave-CISK modes. In linear CISK theories, which necessitate the prescription of a "negative heating" over the low-level moisture divergence regions, short wavelengths are usually most unstable. In both of the numerical studies this preference for small scale is overcome by the nonlinear effect of the positive-only heating CISK parameterization. Instead of exponential growth in the short wavelengths, a channeling of energy into the longest wave components was observed.

The simulated disturbances cannot be considered a neutral Kelvin mode modified by the latent heating. First, the vertical structure of the dominant neutral mode is not significantly modified by the latent heating (Fig. 20 of Lau and Peng 1987), and hence it cannot account for the deep vertical scale of the disturbances obtained in the simulations. Furthermore, a distinct east–west asymmetry and a slight westward tilt are present in the disturbances. Such a structure cannot be explained in terms of a single neutral mode.

The purpose of this paper is to perform a linear analysis, based on the equatorial β-plane wave theory, to elucidate the basic dynamics of the Kelvin wave-CISK. A 5-level model will be used to facilitate the comparison with Lau and Peng's (1987) and Hayashi and Sumi's (1986) numerical results. Through a single mode stability analysis, an attempt will also be made to answer the question of why Rossby modes are not favored. In addition, some analogies between the dynamics and thermodynamics of the Kelvin wave-CISK and Chang's (1977) viscous mode effects will be discussed in the conclusion. Since the linear theory cannot properly treat the effect of positive-only heating, the problem of horizontal scale selection cannot be resolved here. An analytical study of the nonlinear CISK effect is being carried out and the results will be reported in a follow-up paper.

2. Equations

In a linearized multilevel p-coordinate model, the horizontal structure of each of the vertical mode is described by a system of shallow water equations:

$$\frac{\partial u_i}{\partial t} - \beta y v_i + \frac{\partial \phi_i}{\partial x} = 0,$$

$$\frac{\partial v_i}{\partial t} + \beta y u_i + \frac{\partial \phi_i}{\partial y} = 0,$$

$$\frac{\partial \phi_i}{\partial t} + c_i^2\left(\frac{\partial u_i}{\partial x} + \frac{\partial v_i}{\partial y}\right) = Q_i, \tag{1}$$

where $c_i^2 = gh_i$ with h_i being the equivalent depth of the vertical mode. The mass source Q_i is a projection of the heating function $Q(x, y, p, t)$ on the vertical profile $Z_i(p)$ of the vertical mode:

$$Q_i = \frac{c_i^2 R}{c_p}\int_0^{p_s} Z_i \frac{\partial}{\partial p}\left(\frac{Q}{p\sigma_s}\right)dp \Big/ \int_0^{p_s} Z_i^2 dp, \tag{2}$$

where σ_s is the static stability parameter. In a CISK parameterization:

$$Q(x, y, p, t) = -mLq^*_{900}(x, y, t)\omega_{900}(x, y, t)\eta(p)/\rho_{900}, \tag{3}$$

where m is a moisture availability factor, L the latent heat, q^*_{900} and ρ_{900} are the specific humidity and the air density respectively at 900 mb, η the normalized vertical heating profile [$\int_0^{p_s}\eta(p)dp = 1$], and

$$\omega_{900} = \sum_{i=1}^{l}\int_0^{900\text{ mb}} -\left(\frac{\partial u_i}{\partial x} + \frac{\partial v_i}{\partial y}\right)Z_i(p)dp, \tag{4}$$

where the sum is taken over all the l vertical modes. Substituting (4) into (3) and (2) gives

$$Q_i = \sum_{j=1}^{l}\frac{c_i^2 R}{c_p\rho_{900}} mLq^*_{900}\int_0^{900\text{ mb}} Z_i\frac{\partial}{\partial p}\left(\frac{\eta}{p\sigma_s}\right)dp \times\left[\int_0^{900\text{ mb}} Z_j(p)dp\right]\left(\frac{\partial u_j}{\partial x} + \frac{\partial v_j}{\partial y}\right)\left\{\int_0^{p_s} Z_i^2 dp\right\}^{-1} \equiv \sum_{j=1}^{l} K_{ij}\left(\frac{\partial u_j}{\partial x} + \frac{\partial v_j}{\partial y}\right). \tag{5}$$

Considering only Kelvin waves, $v_i = 0$, (1) is further separated into:

$$\frac{\partial u_i}{\partial t} + \frac{\partial \phi_i}{\partial x} = 0,$$

$$\frac{\partial \phi_i}{\partial t} + c_i^2 \frac{\partial u_i}{\partial x} = \sum_{j=1}^{l} K_{ij} \frac{\partial u_j}{\partial x}, \tag{6a}$$

and

$$\beta y u_i + \frac{\partial \phi_i}{\partial y} = 0. \tag{6b}$$

For a single wave component with all variables proportional to $e^{i(kx-\nu t)}$, (6a) reduces to

$$\sum_{j=1}^{l} \{\delta_{ij}(c_j^2 - \nu^2/k^2) - K_{ij}\} = 0 \tag{7}$$

where $i = 1, 2, 3, \cdots, l$ and δ_{ij} is the Kronecker delta.

The value of $c = \nu/k = c_{\mathrm{Re}} + ic_{\mathrm{Im}}$ is to be solved as eigenvalues of (7), subject to the requirement that $c_{\mathrm{Re}} > 0$, so that CISK occurs when $c_{\mathrm{Im}} > 0$.

It is worth noting that any CISK modes that may occur remain nondispersive like the normal Kelvin waves. This means that a localized disturbance may propagate without significant changes of shape over some distance. In a linear analysis, the faster-growing short waves will finally dominate the flow. However, this tendency may be suppressed by the nonlinear effect of CISK. When no negative heating is allowed, the CISK mechanism operates only within the region of ascending motion. This means that while the length scale of the ascending motion region tends to decrease due to the selectivity of the CISK mechanism, the broad region of descending motion remains neutral and its motion is mainly a passive response to the lateral forcing from the ascending region. The resultant motion field will thus have a narrow, concentrated region of ascending motion accompanied by general descending motion elsewhere, resembling the disturbances obtained by Lau and Peng (1987) and Hayashi and Sumi (1986).

3. Kelvin CISK modes and vertical heating profiles

In this section, we shall study the effect of vertical heating profile on Kelvin CISK modes. For easier presentation of the results, we shall discuss in terms of unnormalized heating profiles $\xi_{1000}, \xi_{800}, \xi_{600}, \xi_{400}, \xi_{200}, \xi_0$, where the subscripts denote the pressure level in mb. The normalized heating profiles η_i are given by $\eta_i = \xi_i/(\sum_j \xi_j \Delta_p)$ with Δ_p denoting the thickness of model levels.

In all calculations, $l = 5$, $\xi_{1000} = \xi_0 = 0$ and $\xi_{800} = 1$. Figure 1 shows the effect of varying the vertical heating profile. Figures 1a–b are c_{Re} and c_{Im}, respectively, as a function of ξ_{400} and ξ_{600}, which both range from 0 to 4. Here $\xi_{200} = 0$ and $m = 1$.

Two types of CISK modes are obtained. When the heating is mainly in the lower troposphere, the CISK mode is stationary. When midtropospheric heating becomes stronger, the CISK modes become propagating with speeds ranging from about 15 m s^{-1} when $\xi_{600} > \xi_{400}$ to near 30 m s^{-1} when $\xi_{400} > \xi_{600}$. This pattern is not qualitatively changed by the presence of upper tropospheric heating, as demonstrated by Fig. 1c, which shows c_{Re} for the same range of midlevel heating profiles but $\xi_{200} = 1$.

We will now examine how these two types of CISK modes arise mathematically. This knowledge will help the physical discussion to be given later in section 6. When $m = 0$, $K_{ij} = 0$, the eigenvalues of (7) are simply $c_{\mathrm{Im}} = 0$, $c_{\mathrm{Re}} = \sqrt{gh_i}$. With $m \neq 0$, (5) shows that interactions between the vertical modes lead to changes in the eigenvalues. Figures 2a–c illustrate the typical variation of the eigenvalues with m.

Figure 2a shows that a stationary CISK mode is obtained for $\xi_{200} = \xi_{400} = \xi_{600} = 0.5$. As m increases, the interactions among the vertical modes lead to a slight and gradual decrease of the phase speed of the external mode and the higher internal modes. Thus these modes are not significantly affected by the CISK effect. However, the phase speed of the lowest mode decreases rather rapidly for $m > 0.5$, and at $m \approx 0.96$, the eigenvalue (c^2) of the mode becomes negative, giving rise to a stationary CISK mode ($c_{\mathrm{Re}} = 0$, $c_{\mathrm{Im}} > 0$).

Figure 2b is for a fast CISK mode ($c_{\mathrm{Re}} \approx 30$ m s^{-1}) obtained for $(\xi_{200}, \xi_{400}, \xi_{600}) = (0.5, 2, 0.5)$. This mode is seen to develop mainly from the interaction between the two intermediate internal modes. As m increases, the phase speeds of these two modes approach each other and finally meet at $m \approx 0.82$. For higher values of m, the two neutral modes disappear and are replaced by two modes with complex conjugates c and c^*, i.e., one stable and the other damped.

Figure 2c is for a slow CISK mode ($c_{\mathrm{Re}} \approx 18$ m s^{-1}) obtained for $(\xi_{200}, \xi_{400}, \xi_{600}) = (0.5, 0.5, 2)$. In this case, the mode is seen to evolve mainly from the interaction between the two lowest internal modes.

The above results suggest that the stationary CISK modes arise mainly from the action of CISK on the lowest mode alone, whereas the propagating CISK modes arise mainly from the interactions between two internal modes. These observations will prove useful in a later discussion of the physical interpretation for the structure and the dynamical mechanisms of these CISK modes.

4. Structure of the CISK modes

For easy comparison with Lau and Peng's (1987) results, we construct "solitary waves" of our CISK modes with heating concentrated in a small longitudinal interval by specifying that

$$\omega_{900} = \frac{1}{\sqrt{2\pi}\sigma} \exp\left\{-\frac{x^2}{2\sigma^2}\right\} - 1$$

with $\sigma = 5°$ latitude.

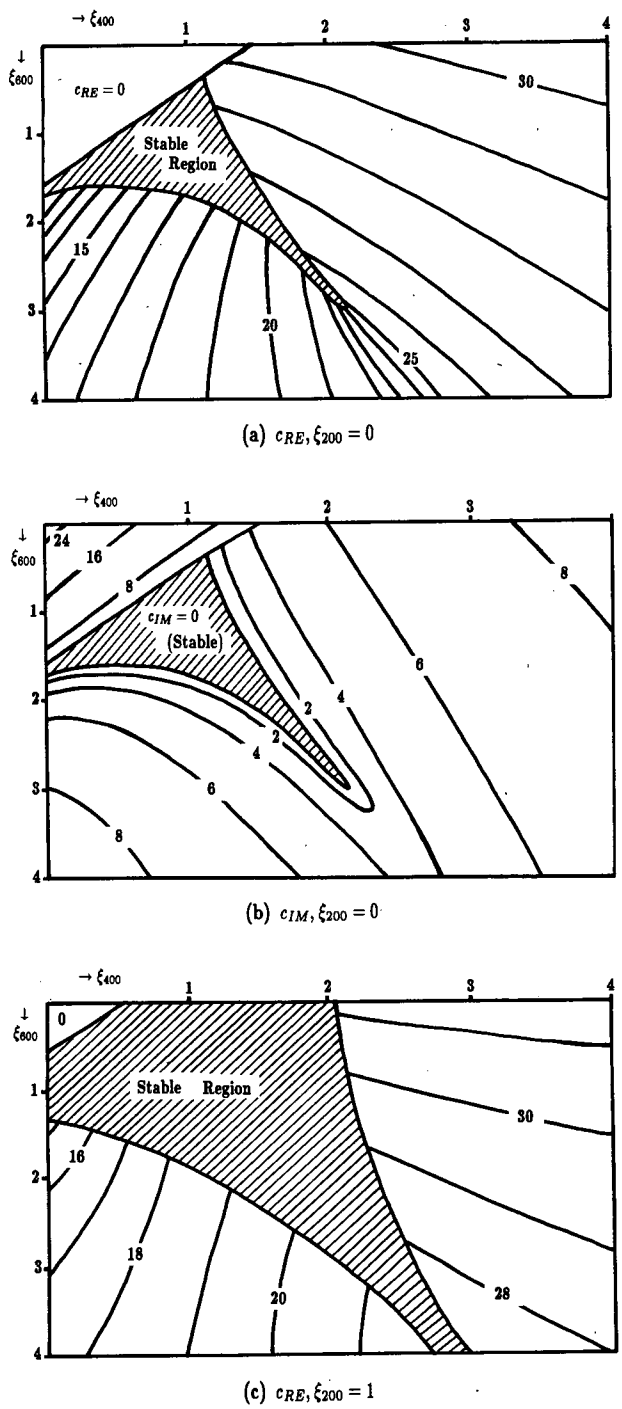

FIG. 1. (a) c_{Re} for $\xi_{200} = 0$; (b) c_{Im} for $\xi_{200} = 0$; and (c) c_{Re} for $\xi_{200} = 1$; as a function of ξ_{400} and ξ_{600}. Unit in m s^{-1}.

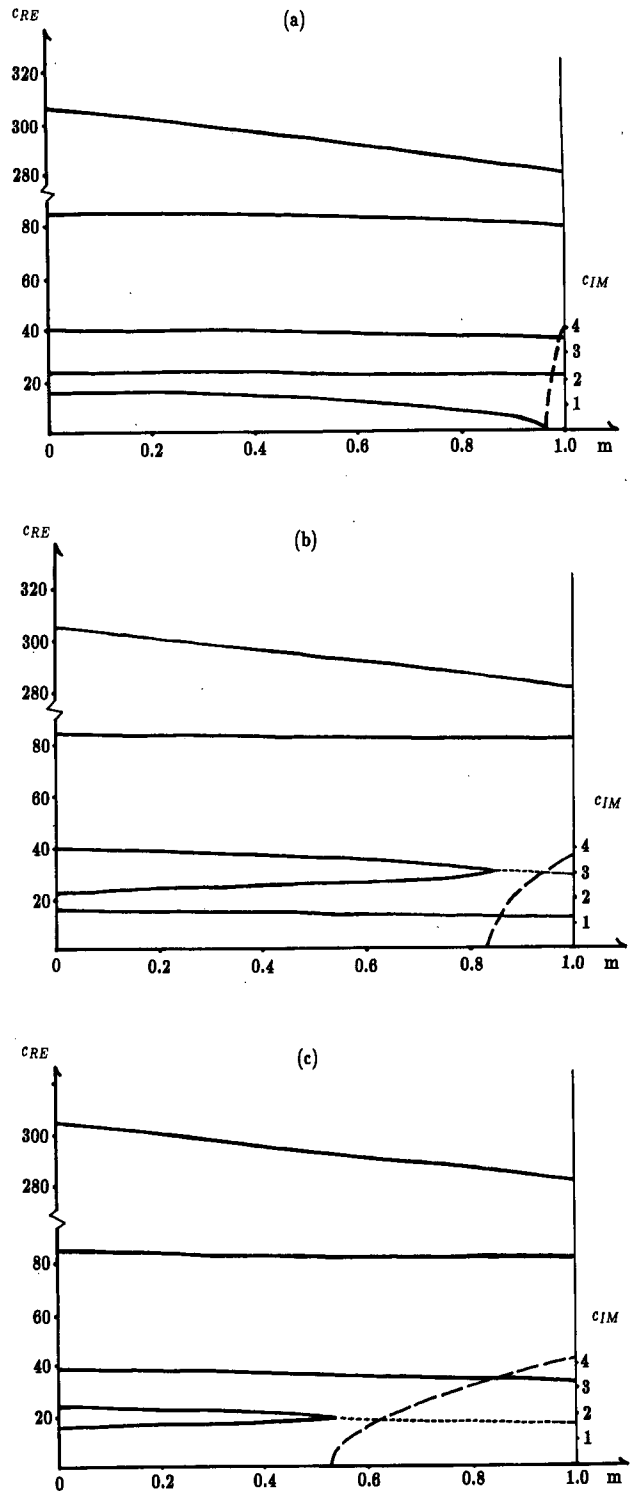

FIG. 2a. The c_{Re} (solid) and c_{Im} (long-dashed) for all vertical modes as a function of m. Heating is maximum at 800 mb. For large m the lowest mode become a stationary CISK mode. (b) As in (a) except heating is maximum at 400 mb. Interaction between two intermediate internal modes leads to a fast CISK mode whose c_{Re} is represented by short dashed line. (c) As in (a) except heating is maximum at 600 mb. Interaction between the lowest two internal modes leads to a slow CISK mode.

Figures 3a–b show the circulations in the equatorial plane of the fast and the slow CISK modes respectively. Some common characteristics may be noted. These propagating modes are asymmetrical to the east and west of the heating region. The circulation to the east is more intense and has a greater depth. A slight west-

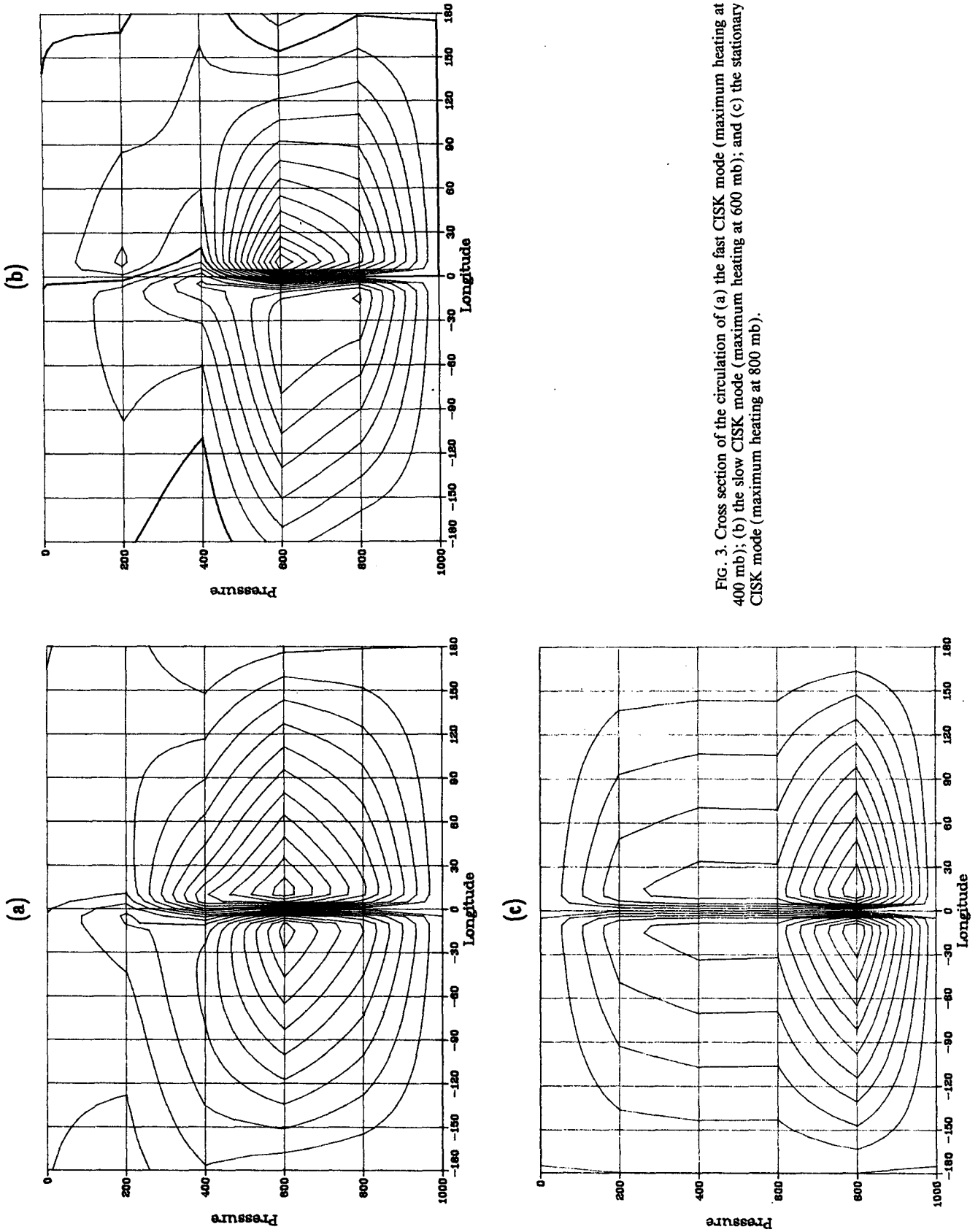

FIG. 3. Cross section of the circulation of (a) the fast CISK mode (maximum heating at 400 mb); (b) the slow CISK mode (maximum heating at 600 mb); and (c) the stationary CISK mode (maximum heating at 800 mb).

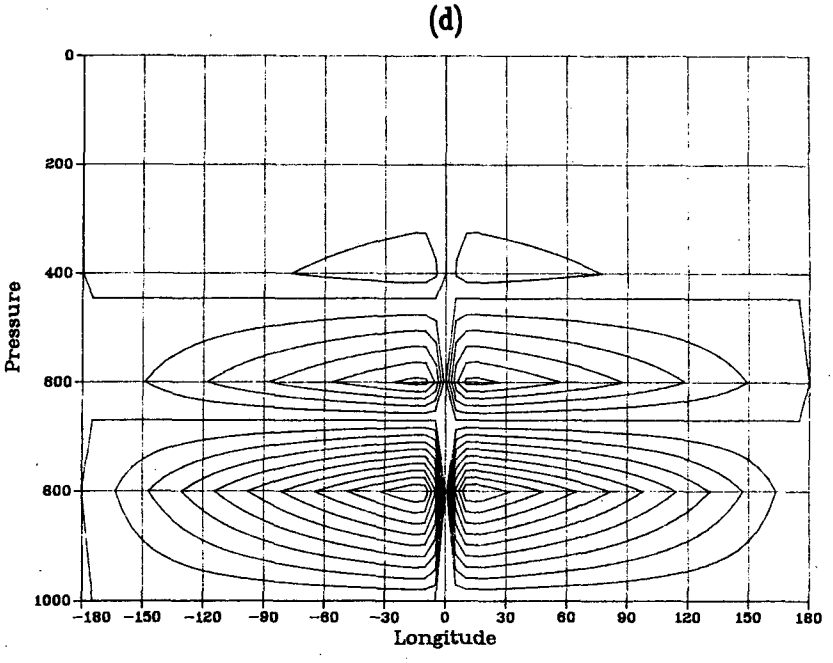

FIG. 3. (*Continued*) (d) The structure of a free Kelvin wave mode which has the same propagation speed (16 m s^{-1}) as the slow CISK mode shown in Fig. 3b.

ward tilt of the system is also observed. The structure of the slow mode bears a clear resemblance to the disturbance obtained by Lau and Peng (1987).

The circulation of a stationary CISK mode is shown in Fig. 3c. This mode is east–west symmetrical to the heating region. The circulation is most intense in the lower troposphere but weak flows persist through middle to upper troposphere.

Figure 3d shows the circulation of the lowest internal free mode of the model. A comparison with Fig. 3b highlights a significant property of the CISK modes. Although both the free mode and the slow CISK mode propagate at about the same phase speed (16 m s^{-1}), the slow CISK mode has a much deeper vertical structure than the free mode. A free mode with a vertical structure closer to that of the slow CISK mode would be expected to propagate at a speed of 30–40 m s^{-1} rather than 16 m s^{-1}. Hayashi and Sumi's (1986) results show that when CISK heating is cut off, the eastward propagating disturbance rapidly develops short vertical wavelength features and speeds up to about 30 m s^{-1} may therefore be explained by an evolution of the slow CISK mode to a free mode as latent heating is cut off.

The horizontal structure of the CISK modes is given by the equations:

$$-cu_i + \phi_i = 0,$$

$$\beta y u_i + \frac{\partial \phi_i}{\partial y} = 0, \quad i = 1, \cdots, 5, \tag{8}$$

which can be readily solved when given the complex value of c. The solution is

$$u_i(y) = u_i(0) \exp\left\{\frac{-\beta y^2}{2c}\right\}$$

$$= u_i(0) \exp\left\{-\frac{\beta c_{\mathrm{Re}} y^2}{2|c|^2}\right\} \exp\left\{\frac{i\beta c_{\mathrm{Im}} y^2}{2|c|^2}\right\}. \tag{9}$$

Adding up the contributions from all five vertical modes, the zonal velocity of a single wave mode is given by

$$u = \sum_{j=1}^{5} \left\{ U_j Z_j(p) \exp\left[-i\left(kx + \frac{\beta c_{\mathrm{Im}} y^2}{2|c|^2} - kc_{\mathrm{Re}} t\right)\right] \times \exp\left[-\frac{\beta c_{\mathrm{Re}} y^2}{2|c|^2}\right] \exp[kc_{\mathrm{Im}} t] \right\}, \tag{10}$$

where U_j represents the components of the normalized eigenvector of (7) corresponding to the complex eigenvalue c.

As was pointed out by Chang (1977), since $c_{\mathrm{Re}}, c_{\mathrm{Im}} > 0$, these CISK modes exhibit a westward phase tilt from the equator which gives rise to a poleward propagation similar to the observed 30–50 day oscillations. Figures 3e and 3f show the horizontal distributions of divergence and u velocity component, respectively, at 900 mb of the slow Kelvin wave-CISK mode shown in Fig. 3b.

5. Dynamical mechanisms of the development of the CISK modes

To gain a deeper insight into the origin of these Kelvin CISK modes, we first consider the effect of CISK

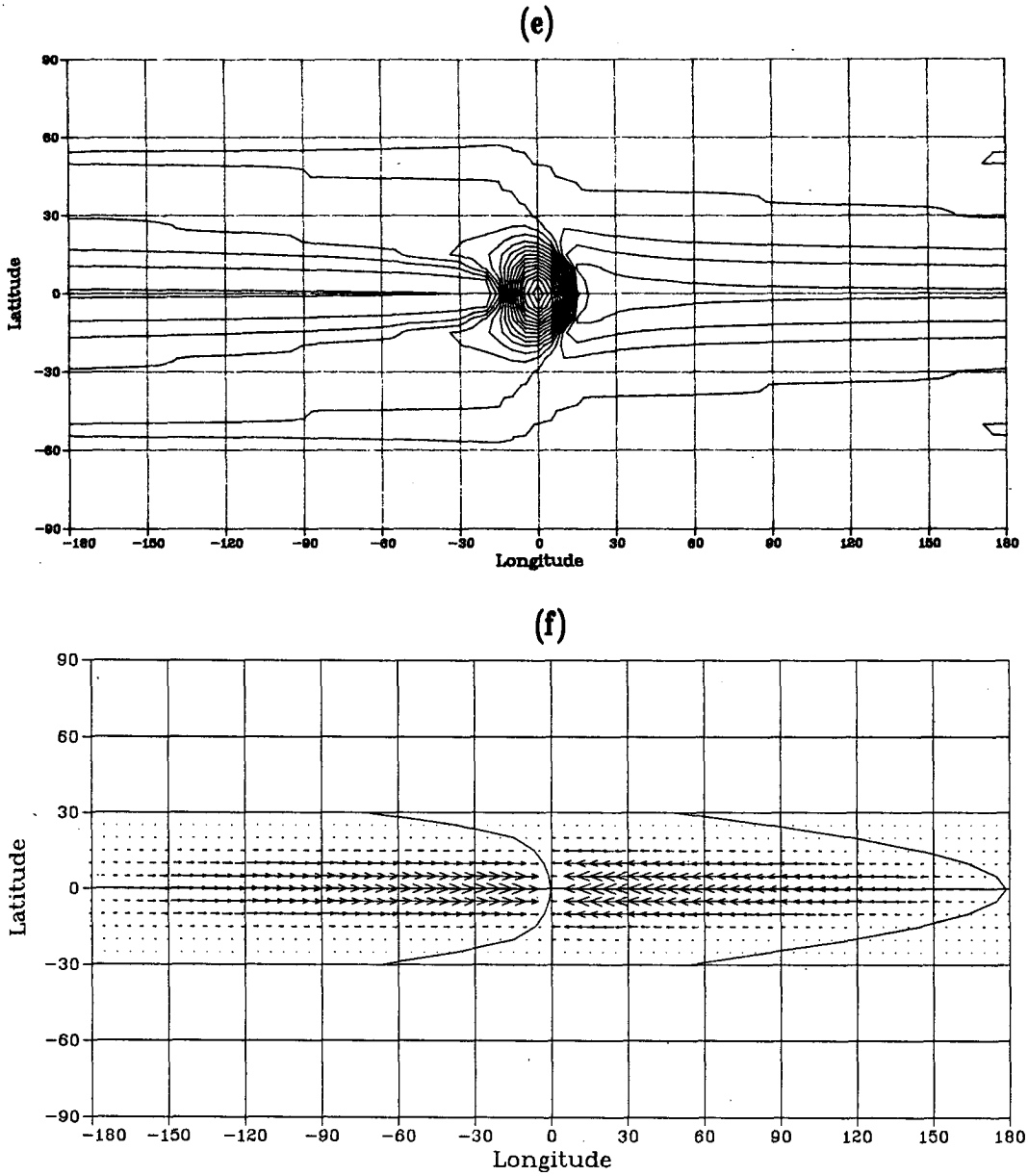

FIG. 3. (*Continued*) The horizontal structure of the slow Kelvin wave-CISK mode shown in Fig. 3b: (e) divergence field at 900 mb; (f) u-component field at 900 mb. The curve marks the zero-u axis.

heating on a single vertical mode. Dropping the subscripts, the equations are

$$\frac{\partial u}{\partial t} - \beta y v + \frac{\partial \phi}{\partial x} = 0,$$

$$\frac{\partial v}{\partial t} + \beta y u + \frac{\partial \phi}{\partial y} = 0,$$

$$\frac{\partial \phi}{\partial t} + c_0^2\left(\frac{\partial u}{\partial x} + \frac{\partial v}{\partial y}\right) = Q = K\left(\frac{\partial u}{\partial x} + \frac{\partial v}{\partial y}\right). \quad (11)$$

Let $c_0 \approx 30$ m s^{-1}, we have a "baroclinic" mode with compensating upper and lower flows. We shall regard the variables in (11) to represent the upper level flow so that $\phi > 0$ means an upper-level high pressure overlying a lower-level low pressure. In order to have CISK, the constant K must be positive.

For small values of K, the effect of CISK heating is seen to cause a reduction of the equivalent depth from c_0^2 to $c_s^2 = (c_0^2 - K)$. All wave modes remain stable but propagate more sluggishly at speeds reduced by a factor of c_s/c_0.

When $K > c_0^2$, $c_s^2 < 0$, unstable modes with zero phase speed arise. In a multilevel model, this instability

mechanism affects most readily the slowest vertical mode which has the smallest c_0^2. This is consistent with our earlier observation in Fig. 2 that the stationary CISK modes arise mainly through the action of CISK on the slowest vertical mode.

The above indicates propagating CISK modes cannot exist in a single vertical mode CISK model such as (11). The reason for this is readily seen in the kinetic energy equation:

$$\frac{d}{dt}\left\langle \frac{1}{2}(u^2+v^2)\right\rangle = \left\langle \phi\left(\frac{\partial u}{\partial x}+\frac{\partial v}{\partial y}\right)\right\rangle \qquad (12)$$

where $\langle\ \rangle$ indicates averaging over the spatial domain.

So long as $c_s^2 > 0$, (11) shows that ϕ and divergence are 90° out of phase and the generation term in (12) averages to zero, indicating that no instability may be expected. So, how do we obtain unstable modes that are propagating?

Davies (1979) studies CISK with a time lag, i.e., the latent heating is assumed to take place at a time lag of Δt after the occurrence of low-level moisture convergence. The plausibility and the observational support of such a time-lag effect was thoroughly reviewed by Davies (1979). We shall not elaborate on this point as it will soon be clear that we are not really going to assume a time lag in our model. However, an examination of the time-lag effect in a single mode model is helpful in establishing certain concepts for explaining how the interactions between the vertical modes of a multilevel model may develop propagating CISK modes.

For a time lag Δt, the heating term may be written as

$$Q(t) = K\int^t \left(\frac{\partial u}{\partial x}+\frac{\partial v}{\partial y}\right)\delta(t-\Delta t-t')dt' \qquad (13)$$

where $\delta(t)$ is the Dirac delta function. A Fourier transform of (11) gives the following equations for a Kelvin wave mode:

$$\begin{aligned} -cu + \phi &= 0, \\ -c\phi + c_0^2 u &= Ke^{ikc\Delta t}u. \end{aligned} \qquad (14)$$

The dispersion relation now becomes

$$c^2 - c_0^2 + Ke^{ikc\Delta t} = 0. \qquad (15)$$

A solution of (15) is presented in Fig. 4. The time lag is assumed to be 12 hours. We see that Kelvin waves of zonal wavenumber larger than 12 become unstable with this time-lag effect. The reason for this occurrence of instability is easily explained using Fig. 5. For a small time lag, the wave is generally damped as the heating associated with (upper) divergence will fall in areas of negative ϕ. However, at larger lag, the heating will fall back far enough to act on regions of positive ϕ which means energy generation.

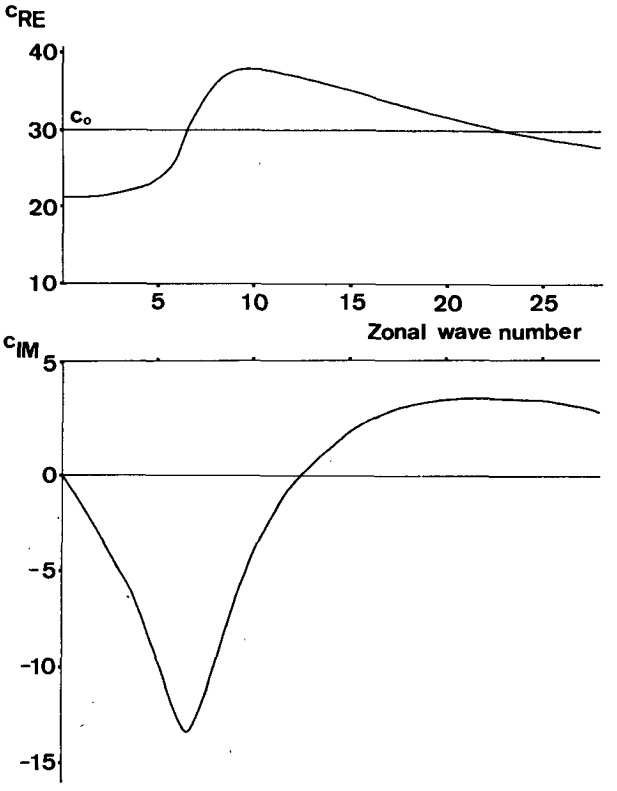

FIG. 4. The c_{Re} and c_{Im} for Kelvin waves in a single vertical mode model with a time-lagged CISK parameterization. Δt = 12 h, c_0 = 30 m s^{-1}.

It is clear that the motions obtained by Lau and Peng (1987) and Hayashi and Sumi (1986) are not time-lagged CISK, single vertical modes. First, there was no time-lag effect in their latent heat parameterization. Furthermore, single vertical mode models cannot account for the east–west asymmetry of their eastward propagating disturbances.

Nevertheless, the above analysis provides a clue to the mechanism of Kelvin wave-CISK in multilevel models. When the latent heating parameterization does not include a time-lag effect, instability may still occur if the interactions between the various vertical modes give rise to the required phase shift between heating and geopotential. Consider the Kelvin waves of various vertical modes excited by a local disturbance. After some time, the faster vertical mode waves would have propagated ahead of the slower vertical mode waves. The lower level flow and its associated moisture convergence, in general, are more strongly influenced by the slower vertical modes. For the faster vertical modes, there is thus a lag of the heating region with respect to its divergence field and hence a possibility for instability to occur. With appropriate amplitude ratio and relative phase shift between the faster and the slower vertical modes, the two modes may lock together into a propagating CISK mode.

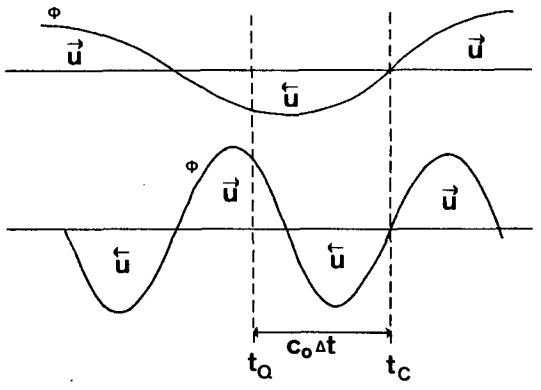

FIG. 5. Schematic diagram showing the destabilization of short Kelvin waves by the time-lagged CISK. t_C denotes the time of moisture convergence associated with the upper level divergence as shown in the figure. The t_Q denotes the time of latent heating which is delayed by Δt. For long waves (upper curve), the heating occurs in region of negative ϕ, and leads to damping. For short waves (lower curve), heating occurs in region of positive ϕ and results in instability.

The above explanation of instability through vertical mode interactions agrees well with the propagating Kelvin CISK modes obtained in the multilevel model. First, the propagation speed of the CISK mode may be expected to be between those of the two interacting vertical modes, which is consistent with Figs. 2b–c. Furthermore, the characteristics of the faster (slower) vertical mode may be expected to be prominent ahead of (behind) the heating region. This explains the asymmetrical structure of a deeper vertical scale to the east of the heating region and a shallower vertical scale to the west.

6. Stability of Rossby waves

Equations (1)–(5) do not allow a simple analysis of the Rossby wave CISK in a multilevel model. However, the analogy between the vertical mode interaction effect and the time-lag effect provides a quick way to check tentatively the stability of Rossby waves.

For Rossby waves with a time lag in latent heating, the equation for the meridional velocity component is

$$\frac{\partial^2 v}{\partial \zeta^2} + \left\{ \frac{\nu^3 - k(\beta + \nu k)(c_0^2 - K\tilde{w})}{\beta\nu(c_0^2 - K\tilde{w})} c_0 - \frac{c_0^2 \zeta^2}{c_0^2 - K\tilde{w}} \right\} v = 0, \quad (16)$$

where $\zeta = \sqrt{\beta/c_0}\, y$ and $\tilde{w} = e^{i\nu\Delta t}$.

Expanding v in terms of the Hermite functions $\Psi_n = e^{-\zeta^2/2} H_n(\zeta)$:

$$v = \sum_{n=0}^{\infty} v_n \Psi_n(\zeta),$$

we reduce (16) to the following recurrence relation between the coefficients v_n:

$$\tfrac{1}{4} A v_{n-2} + \left[(2n+1)\left(1 + \frac{A}{2}\right) - B \right] v_n + (n+1)(n+2) A v_{n+2} = 0, \quad (17)$$

where $A = K\tilde{w}/(c_0^2 - K\tilde{w})$, $B = [\nu^3 - k(\beta + \nu k)(c_0^2 - K\tilde{w})]/[\beta\nu(c_0^2 - K\tilde{w})]c_0$.

A truncated system of (17) may be solved using an iterative procedure. In all the cases attempted, Rossby waves are found to be stable to the time-lag CISK effect. As an example, Fig. 6 shows the result of our computation for the gravest Rossby mode. For all wavelengths, the time-lag CISK effect is seen to be damping and to reduce the propagation speed.

7. Effect of vertical resolution on the Kelvin CISK modes

The CISK modes of sections 3 and 4 were computed using a 5-level model. The model was chosen to correspond to that used by Lau and Peng (1987) so that a direct comparison of the theoretical CISK modes and their simulation results may be made. In this respect, the theory appears to have been successful in accounting for some main characteristics of Lau and Peng's results.

A 5-level model is often adequate for representation of many deep atmospheric circulation systems. How-

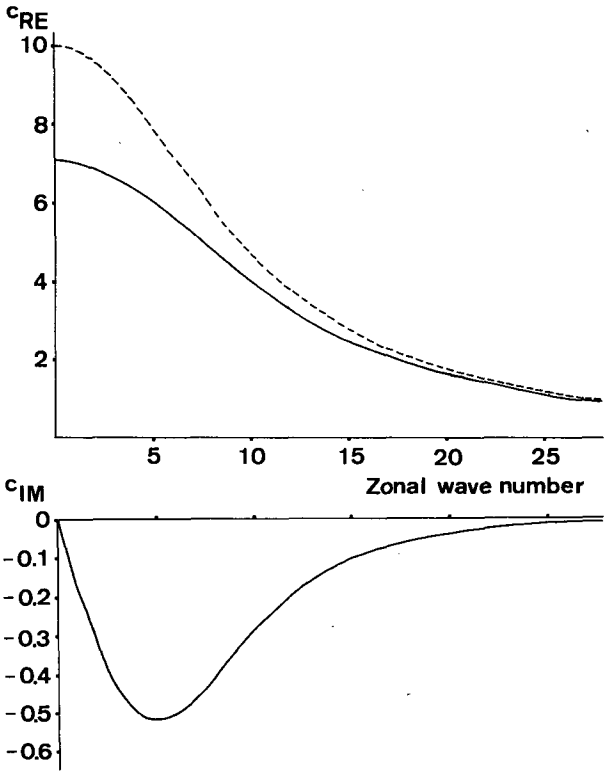

FIG. 6. As in Fig. 4 except for the gravest Rossby wave mode.

ever, it is of rather coarse resolution. There may therefore be some doubt as to the robustness of the CISK modes—are they spurious results of the finite difference model, and will there be significant changes in the unstable modes as more vertical levels (and hence more vertical modes) are added?

To answer such questions, the stability of a 20-level model was examined by solving the corresponding eigenvalue problem (7). Results of this study confirmed that our conclusions drawn from a 5-level model remain valid for models with higher vertical resolutions. A typical example is presented in Table 1.

The case presented in Table 1 has a heating profile with $\xi_{1000} = 0$, $\xi_{800} = 1$, $\xi_{600} = 2$, $\xi_{400} = 1$ and $\xi_{200} = 0$. At the other levels of the 20-level model, the required ξ were obtained using Lagrange interpolation. Figures 1a and 1b show that the corresponding 5-level model has a slow CISK mode with $c_{Re} \approx 17$ m s^{-1} and $c_{Im} \approx 4$ m s^{-1}. Table 1 shows that in the 20-level model, an unstable mode develops when m becomes larger than 0.6. As m increases from 0.7 to 1, the unstable mode's c_{Re} decreases from about 16 m s^{-1} to about 14.5 m s^{-1}, while its c_{Im} increases from 0 to about 5.5 m s^{-1}. These figures compare well with the corresponding figures of the 5-level model.

In all cases analyzed, similar correspondence and agreement between the 20-level and 5-level results was obtained. The CISK modes of the 5-level model therefore appear to be robust to an increase in model resolution and hence are unlikely spurious results of a crude model. It is, however, clear that the coarse vertical resolution of a 5-level model has given rise to small distortions in the values of c_{Re} and c_{Im}. Fortunately, the distortions were observed to be small in all cases studied (within 15%) and did not lead to any significant change in the overall structure of the CISK modes.

TABLE 1. Occurrence of a slow Kelvin CISK mode in a 20-level model with a heating profile defined by specifying $\xi_{800} = 1$, $\xi_{600} = 2$, $\xi_{400} = 1$, $\xi_{200} = 0$, and ξ at other levels obtained by Lagrange interpolation.

$m = 0.6$		$m = 0.7$		$m = 0.8$		$m = 0.9$		$m = 1.0$	
c_{Re}	c_{Im}	c_{Re}	c_{Im}	c_{Re}	c_{Im}	c_{Re}	c_{Im}	c_{Re}	c_{Im}
296.0	0	293.8	0	291.5	0	289.2	0	286.9	0
162.5	0	162.5	0	162.6	0	162.6	0	162.7	0
66.4	0	66.2	0	66.1	0	66.0	0	65.9	0
41.6	0	41.0	0	40.5	0	40.0	0	39.6	0
26.1	0	25.4	0	24.8	0	24.2	0	23.7	0
17.2	0	15.8	1.5	15.3	3.1	14.9	4.4	14.6	5.7
15.6	0	15.8	−1.5	15.3	−3.1	14.9	−4.4	14.6	−5.7
13.6	0	14.2	0	14.6	0	14.8	0	14.8	0
11.7	0	12.2	0	12.5	0	12.7	0	12.8	0
9.2	0	9.3	0	9.4	0	9.5	0	9.5	0
7.6	0	7.6	0	7.6	0	7.7	0	7.7	0
6.5	0	6.5	0	6.5	0	6.5	0	6.5	0
5.8	0	5.8	0	5.8	0	5.8	0	5.8	0
5.4	0	5.4	0	5.4	0	5.4	0	5.4	0
5.2	0	5.2	0	5.2	0	5.2	0	5.2	0
4.9	0	5.0	0	5.0	0	5.1	0	5.1	0
4.3	0	4.4	0	4.4	0	4.4	0	4.4	0
3.8	0	3.8	0	3.8	0	3.8	0	3.8	0
3.4	0	3.4	0	3.4	0	3.4	0	3.4	0
2.7	0	2.7	0	2.7	0	2.7	0	2.7	0

8. Summary and conclusions

Using a linearized, multilevel equatorial β-plane model, the effect of latent heating forced by low-level convergence was investigated. The main findings are

1) The latent heating induces an interaction between the vertical modes. Except for a slight reduction of phase speeds, the external mode and higher internal mode Kelvin waves are not significantly affected. For the lower modes, the effect may lead to the occurrence of CISK modes.

2) Depending on the vertical heating profile, two types of CISK modes may occur. For heating with a maximum in the lower troposphere, the instability arises from the action of latent heating on the lowest internal mode. In physical terms, the heating may be considered to have destroyed the "static stability" for the lowest internal mode. This unstable mode is stationary, east–west symmetrical, and has a deeper vertical scale than the free lowest internal mode.

3) For heating with a maximum near the midtroposphere, the CISK modes are eastward propagating with a phase speed between 15–30 m s^{-1}. These modes arise from the interaction between two internal modes, when the slower mode generates a heating in-phase with the thickness field of the faster mode. Consequently, the characteristics of the faster (slower) mode is manifested ahead of (behind) the heating region, resulting in an asymmetric structure in the east–west direction and a slight westward phase tilt with height. These modes bear a clear resemblance to the disturbances obtained by Lau and Peng (1987).

4) An analysis of the time-lagged CISK, single vertical-mode model indicates that Rossby waves in a multilevel model are probably not susceptible to the instability of the Kelvin CISK modes. However, this conclusion is tentative and needs to be verified by rigorous analysis.

Based on these findings, we may conclude that Kelvin CISK modes in multilevel models provide a satisfactory interpretation of the disturbances obtained by Lau and Peng (1987) and Hayashi and Sumi (1986). However, we have to explain the lack of growth in their simulated disturbances. This is probably due to a combination of two factors: damping and the nonlinear effect of CISK parameterization. Weakly unstable modes might be maintained in a steady state by dissipative effects. Lau and Peng (1987) showed that the nonlinear CISK parameterization strongly inhibits growth of short waves by channeling their energy to the long waves. This is an important observation and

a thorough theoretical study of this effect should lead to significant insight in tropical dynamical processes.

Since Chang (1977) (see also Stevens and White 1979; Chang 1979) obtained a viscous Kelvin mode solution which resembles the observed 30–50 day oscillations, it may be interesting to compare his solution, which may be viewed as a mild wave-CISK mode, with the Kelvin wave-CISK modes studied here. Chang (1977) showed that in the normal Kelvin waves a deep vertical structure necessitates a relatively fast phase speed in order for the inertial acceleration to balance the generation. When viscous effects become important, the main balance is shifted to between heating and damping such that the inertial acceleration due to phase propagation is small. This character is mathematically manifested by a significant imaginary part of the phase speed, and it also produces the observed poleward propagation. The same reasoning may be useful in considering the thermodynamics and dynamics of the Kelvin wave-CISK modes. Here, instead of being balanced entirely by the acceleration due to propagation, a portion of the heating energy is removed by the wave growth (which is also represented by an imaginary phase speed). This causes a shift of the phase between temperature and vertical velocity such that potential–kinetic energy conversions become possible. Therefore, the Kelvin waves are subject to a modification which is similar to the viscous effect, giving rise to a slower propagation speed with a deep vertical structure. This effect is in addition to the reduction of the static stability.

Similarly, Chang's (1977) analysis of the difference in force balances between the fast and slow modes may also shed light on the mechanism of Kelvin wave-CISK. Due to the instability, the balance in the momentum equation is modified such that a portion of the pressure gradient force is used for growth, rather than entirely for phase propagation. These unstable modes therefore have u and ϕ fields that are out of phase, resulting in a slower zonal propagation than the free Kelvin waves whose u and ϕ are perfectly in phase. In fact, if the waves are to maintain a steady-state amplitude, dissipation processes and the short- to long-wave energy transfer due to nonlinear effect of CISK must balance the growth due to generation. In this respect, it is not surprising to see that the wave-CISK modes contain some characteristics of the viscous modes. However, since the growth rates are small and the real phase speed is still relatively large, the linear Kelvin wave-CISK modes in the present model are modified only partially by Chang's "viscous effect".

Thus we may draw the following conclusions regarding the slow speed of the propagating Kelvin wave-CISK modes:

1) The development mechanism appears to be the interaction between vertical modes, whereby a deeper internal mode may be "slowed down" when it is locked in with a shallower mode in the 5-level model. (For higher resolution models, more than two vertical modes may be involved in this interaction.)

2) From the point of view of force and energy balances, the meridional, vertical and time scales of these modes are influenced by a growth effect which is analogous to the viscous effect discussed by Chang (1977). This effect, in combination with a reduced static stability, gives rise to a smaller propagation speed.

Our result also suggests that it is unlikely for the 30–50 day oscillations to be excited solely by an interaction with the stationary oscillations of the basic state. Even though the stationary oscillations may, for various possibilities, provide a 30–50 day periodicity, eastward propagating disturbances so excited will necessarily have very shallow vertical structure without the wave-CISK mechanism. Further, in a linear model, the projection of a normal heating profile (with a vertical scale comparable to the depth of the troposphere) onto these shallow modes will be extremely small. This means that any such propagating wave response to 30–50 day forcings will probably be of negligible amplitude.

At the close of this paper, we wish to place our theory in a proper perspective. By isolating the Kelvin mode with the condition $v = 0$, we succeeded in identifying the basic mechanism of the disturbances obtained by Lau and Peng (1987) and Hayashi and Sumi (1986). Kelvin wave-CISK modes have the correct propagation velocity and overall structure. However, it is also not surprising to find features of simulated and observed 30–50 day oscillations that are not present in the Kelvin wave-CISK modes. One example is the Rossby wavelike features (Madden 1986). In the real atmosphere and numerical models, the CISK heating is a "positive-only" nonlinear mechanism. The energy source is concentrated within the narrow region of ascending motion. The broad region of descending motion responds passively to the lateral forcing from the CISK region. The CISK dynamics determine the propagation speed and overall structure. But the total disturbance must also have a weaker flow pattern representing the response of the broad passive descending region to the concentrated heat source. The structure of this secondary flow may be inferred from Lim and Chang's (1983) results for "baroclinic" responses in an easterly mean wind. This implies that some Rossby wave characteristics may be expected to trail behind the Kelvin wave-CISK mode in the total structure of the disturbances. These Rossby wave features are locked onto the mobile latent heating region and are dragged along eastward against their natural tendency to propagate westward. The pattern observed by Madden (1986) can be explained in terms of a Kelvin wave-CISK mode distorted by possibly a sea surface temperature maximum south of the equator. The asymmetrical and eastward propagating Rossby wavelike pattern are readily accounted for from this point of view.

Many important factors that may have significant effect on Kelvin wave-CISK remain to be investigated. Vertical wind shear will possibly cause a deepening of the vertical structure of wave-CISK modes (Lim and Chang 1986). The sensitivity of the wave-CISK modes to the vertical resolution of the model also requires further study. But the most important of all is certainly the "positive-only" nonlinear effect on the scale selection of the wave-CISK mechanism. A deeper understanding of this effect will have wide implication on theories of tropical weather systems where latent heating is a main source of energy.

Acknowledgments. This work was supported by the National Science Foundation (Division of Atmospheric Sciences Grants ATM 8315175 and ATM 8711015, and Division of International Programs). We wish to thank Dr. Li Peng who corrected a few mistakes in the original manuscript and Dr. Rolando R. Garcia for suggesting the inclusion of the 20-level stability analysis results.

REFERENCES

Anderson, J. R., 1984: Slow motions in the tropical troposphere. Atmos. Sci. Pap. No. 381, Colorado State University.

——, and D. E. Stevens, 1986: The presence of linear wavelike modes in a zonally symmetric model of the tropical atmosphere. *J. Atmos. Sci.*, **44,** 2115–2127.

Chang, C.-P., 1977: Viscous internal gravity waves and low-frequency oscillations in the tropics. *J. Atmos. Sci.*, **34,** 901–910.

——, 1979: Reply to comments on "Viscous internal gravity waves and low-frequency oscillations in the tropics." *J. Atmos. Sci.*, **36,** 547.

Davies, H. C., 1979: Phase-lagged wave-CISK. *Quart. J. Roy. Meteor. Soc.*, **105,** 323–353.

Garcia, R. R., and M. L. Salby, 1987: Transient response to localized episodic heating in the tropics—Part II: Far-field behavior. *J. Atmos. Sci.*, **44,** 499–530.

Goswami, B. N., and J. Shukla, 1984: Quasi-periodic oscillation in a symmetric general circulation model. *J. Atmos. Sci.*, **42,** 20–37.

Hayashi, Y.-Y., and A. Sumi, 1986: The 30–40 day oscillations simulated in an "aqua planet" model. *J. Meteor. Soc. Japan,* **64,** 451–467.

Krishnamurti, T. N., and D. Subrahmanyam, 1983: The 30–50 day mode at 850 mb during MONEX. *J. Atmos. Sci.*, **39,** 2088–2095.

——, P. K. Jayakumar, J. Sheng, N. Surgi and A. Kumar, 1985: Divergent circulations on the 30–50 day time scale. *J. Atmos. Sci.*, **42,** 364–375.

Lau, K. M., and P. H. Chan, 1985: Aspects of the 40–50 day oscillation during northern winter from outgoing longwave radiation. *Mon. Wea. Rev.*, **113,** 1889–1909.

——, and ——, 1986: Aspects of the 40–50 day oscillation during northern summer as inferred from outgoing longwave radiation. *Mon. Wea. Rev.*, **114,** 1354–1367.

——, and L. Peng, 1986: Origin of low frequency (intraseasonal) oscillations in the tropical atmosphere. Part I. The basic theory. *J. Atmos. Sci.*, **44,** 950–972.

Lim, H., and C.-P. Chang, 1983: Dynamics of teleconnections and Walker circulations forced by equatorial heating. *J. Atmos. Sci.*, **40,** 1897–1915.

——, and ——, 1986: Generation of internal- and external-mode motions from internal heating: Effects of vertical shear and damping. *J. Atmos. Sci.*, **43,** 948–957.

Lindzen, R. S., 1967: Planetary waves on beta planes. *Mon. Wea. Rev.*, **95,** 441–451.

Madden, R. A., 1986: Seasonal variations of the 40–50 day oscillation in the tropics. *J. Atmos. Sci.*, **43,** 3138–3158.

——, and P. R. Julian, 1971: Detection of a 40–50 day oscillation in the zonal wind in the tropical Pacific. *J. Atmos. Sci.*, **28,** 702–708.

——, and ——, 1972: Description of global-scale circulation cells in the tropics with a 40–50 day period. *J. Atmos. Sci.*, **29,** 1109–1123.

Maruyama, T., 1982: Upper tropospheric zonal wind oscillations with a 30–50 day period over the Equatorial Western Pacific observed in cloud movement vectors. *J. Meteor. Soc. Japan,* **60,** 172–182.

Murakami, T., and T. Nakazawa, 1985: Tropical 45 day oscillation during the 1979 northern hemispheric summer. *J. Atmos. Sci.*, **42,** 1107–1122.

——, —— and J. He, 1984: On the 40–50 day oscillation during the 1979 Northern Hemispheric summer. Part 1. Phase propagation. *J. Meteor. Soc. Japan,* **62,** 440–468.

Salby, M., and R. Garcia, 1987: Transient response to localized episodic heating in the tropics. Part 1: Excitation and short-time near field behavior. *J. Atmos. Sci.*, **44,** 458–498.

Stevens, D. E., and G. H. White, 1979: Comments on "Viscous internal gravity waves and low frequency oscillations in the tropics." *J. Atmos. Sci.*, **36,** 545–546.

Webster, P. J., 1983: Mechanics of monsoon low frequency variability: Surface hydrological effects. *J. Atmos. Sci.*, **40,** 2110–2124.

Yamagata, T., and Y. Hayashi, 1984: A simple model for the 30–50 day oscillation in the tropics. *J. Meteor. Soc. Japan,* **60,** 709–717.

Yasunari, T., 1979: Cloudiness fluctuations associated with the northern hemisphere summer monsoon. *J. Meteor. Soc. Japan,* **57,** 227–242.